Modified Dynamic Time Warping with a Reference Path for Alignment of Repeated Drive-Tests

Vaclav Raida, Philipp Svoboda, Markus Rupp
Institute of Telecommunications
Technische Universität Wien
Vienna, Austria
{firstname.lastname}@tuwien.ac.at

***Abstract*—To provide reliable estimates of wireless network performance along a specific route, repeated measurements should always be conducted to determine the consistency and stability of the relevant key parameter indicators. If the same speed profile cannot be guaranteed during each repetition, then the alignment of the measured signals becomes a challenging task. To tackle this problem, we introduce the concept of the reference path and propose a modified dynamic time warping algorithm. By combining both ideas, we obtain a novel RP-DTW algorithm (modified dynamic time warping with a reference path) that aligns repeated measurements optimally. To demonstrate its usefulness, we apply the algorithm to measurements of received signal power in operational LTE networks of three Austrian operators, which we collected while being onboard a train that traverses between Vienna and Gmünd. We publicly offer our measurements as an open dataset.**

***Index Terms*—dynamic time warping, machine learning, reference path, repeatability, spatial, coordinates, cellular, mobile, network, measurement, LTE, 5G, signal power, RSRP, dataset**

I. Introduction

In operational cellular mobile networks, the analysis of key parameter indicators (KPIs) along particular routes is crucial for understanding the performance experienced by end-users, who walk through a specific street-canyon, drive on a motorway, or travel onboard a train. To make qualified statements about the individual KPIs and investigate their time- and location-dependent statistical properties, repeated measurements along the examined paths are necessary.

With identical speed-profile in each measurement round, we would obtain perfectly aligned time-series: The same relative time would imply the same geographic location in all traces. However, in most scenarios, the speed profile is impacted by uncontrollable influences such as current traffic density, or (in pedestrian measurements) by the impossibility to precisely maintain a predefined velocity.

With GPS measurements at hand, we can calculate the traveled distance for each KPI sample. Still, due to the cumulative nature of the estimated traveled distance, the signals from repeated drives drift apart as even the tiniest GPS location errors sum up with increasing drive-length.

In this paper, we solve the problem of optimally aligning samples from repeated measurements conducted with different speed profiles along a predefined path by modifying a well-known machine learning algorithm—the dynamic time warping (DTW). Our RP-DTW algorithm (modified dynamic time warping with a reference path) is optimum in the sense that it minimizes a distance function between the predefined reference path and the reported measured (GPS) path. RP-DTW aligns M sequences of length L with complexity $O(L^2M)$.

We apply the RP-DTW to repeated railway-measurements of signal strength in operational LTE networks of three Austrian mobile network operators (MNOs). Our measurements are publicly available as an open dataset [1].

A. Related Work

DTW was first introduced in the 1960s and has since been extensively applied to speech recognition. Likewise, DTW has been very successful in data mining and machine learning: for classification, clustering, anomaly detection, and image and video analysis, to name just a few applications [2], [3]. Despite the simplicity of DTW, comparative studies [4], [5] conclude that DTW is hard to beat, and that it can outperform many recent time-series classification algorithms.

In classification, DTW is used mainly as a distance measure, which quantifies the similarity of two sequences. In our work, we are more interested in the aligned sequences themselves, which allow for subsequent analysis of, e.g., the variability of the measured spatial functions. Optimum alignment of M sequences of length L has complexity $O(L^M)$ [6], which is not feasible for more than just a few repetitions.

To circumvent the complexity limitation, researchers have developed heuristic sequence averaging techniques with DTW barycenter averaging [7], [6] being the most prominent one. However, our goal is to obtain multiple aligned sequences and not only a single average sequence.

By introducing additional a-priori knowledge of a reference path and by modifying the DTW constraints, we can optimally align each sequence to the reference path separately. As such, we obtain the complexity $O(L^2M)$ without resorting to approximations or heuristic methods.

Except for [8], which adjusts traces by maintaining the same speed in every round, we are not aware of any paper that would consider the alignment of repeated drives. Mobile measurements in operational networks [9]–[14] either contain a single repetition for each route or compare only cumulative distribution functions of multiple repetitions. A high-granular spatiotemporal representation of multiple repeated measurements synchronized for each space-coordinate is missing.

B. Paper Outline

In Section II, we start with a practical example that illustrates the problem of repeated measurement alignment. In Section III, we mathematically formalize the concept of a spatial function measured along a known path.

Section IV explains the RP-DTW algorithm. Although the classical DTW is well-known, we formulate it in Appendix A to establish the notation consistent with Section IV, which allows to clarify our modifications and highlight the similarities and differences between the classical DTW and RP-DTW.

In Section V, we present our measurement setup, apply the RP-DTW on the signal strength measurements in cellular mobile networks, and analyze the measurement results. In Section VI, we conclude the paper, discuss the limitations of our novel RP-DTW algorithm, and outline future work.

II. A Practical Motivating Example

Let us consider measuring a quantity of interest (in our case, RSRP[1] in an LTE network) along a particular path. We repeat the measurement several times in order to verify whether the target function is time-invariant, to detect anomalies, or to reduce the noise by aggregating multiple samples per location.

Fig. 1 depicts a map of the railway where we performed two drive tests while traveling onboard a train. We see that both drive tests have significantly different speed profiles. In most real-world scenarios, we have to obey traffic rules; thus, it is impossible to have identical speed profiles for all repetitions.

Due to the different speed profiles, the repeated measurements barely overlap when we plot them with respect to relative time in Fig. 2 (a). The same relative time can correspond to a different geographic location in each repetition.

It seems more reasonable to represent the measured signals with respect to the traveled distance in Fig. 2 (b). The measurement equipment usually cannot access the vehicle's odometer; thus, we have to estimate the distance from the GPS location measurements. However, despite the arbitrarily high GPS precision, the measured signals slowly diverge due to the cumulative nature of the calculated distance. Even the tiniest GPS error contributions accrue; hence, we can see in Fig. 2 (b2) that after traveling a sufficiently long distance, both signals become severely mismatched.

Up to this point, we have not leveraged on the prior knowledge of the measurement path (here, the railway between Vienna and Gmünd). The measurement path is usually planned (thus, known beforehand) as we decide where to measure. As explained in Section IV, the additional information about the reference path allows to apply RP-DTW, which achieves an optimum alignment of the repeated RSRP measurements regardless of the traveled distance, see Fig. 2 (c).

III. Problem Statement

A measurement procedure delivers a series of time stamps t_n, function values $\boldsymbol{f}_n$, and locations $\boldsymbol{x}_n$, with $n = 0, \dots, N$. In repeated measurements, the speed profiles may differ as

[1]Reference signal received power [15].

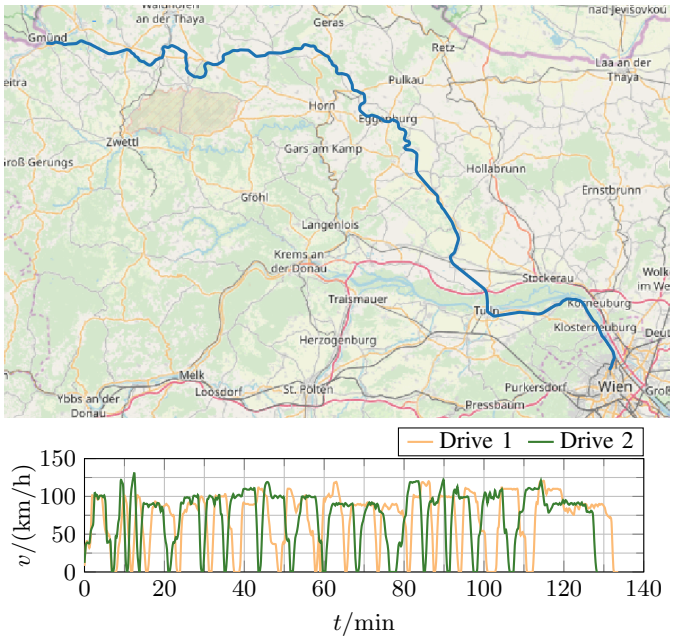

Fig. 1. Railway from Vienna to Gmünd and the speed profiles of two repeated drives. The time on the x-axis is relative to the measurement start.

in Fig. 1; therefore, the relative time stamps correspond to different locations [Fig. 2 (a)]. We thus need to estimate the unknown distances d_n that correspond to the samples $(t_n, \boldsymbol{x}_n, \boldsymbol{f}_n)$ in order to align multiple repetitions.

A. Naive Approach: Summing Coordinate Distances

A straightforward way of estimating the traveled distance d_n that corresponds to the n-th sample $\boldsymbol{f}_n$ is by summing up the distances between the measured coordinates:[2]

$$\hat{d}_n = \sum_{i=0}^{n} \|\boldsymbol{x}_i - \boldsymbol{x}_{i-1}\|_2. \tag{1}$$

The main problem in (1) is that the estimated distance $\hat{d}_n$ is cumulative. Although the GPS coordinates in our railway scenario are very precise and although both repetitions at the beginning of Fig. 2 (b) are aligned accurately, the repeated measurements still slowly drift apart as small location errors accumulate.

B. Sampling Along a Known Reference Path

In most practical measurement campaigns, we plan the path that we are going to measure. We call this a-priori known route "reference path", and we denote it by q. As we will see in Section IV, we can use the knowledge of the reference path q to align repeated spatial measurements.

Formally, let $q \subset \mathbb{R}^D$ be a path of length $d_{\max}$. Each point of q corresponds to a distance $d \in [0, d_{\max}]$; d is the length of a path segment from $q(0)$ to $q(d)$. The path q is continuous,

$$q(d) \colon [0, d_{\max}] \to \mathbb{R}^D. \tag{2}$$

[2]We define an arbitrary reference location $\boldsymbol{x}_{-1}$, from which we measure the cumulative distance.

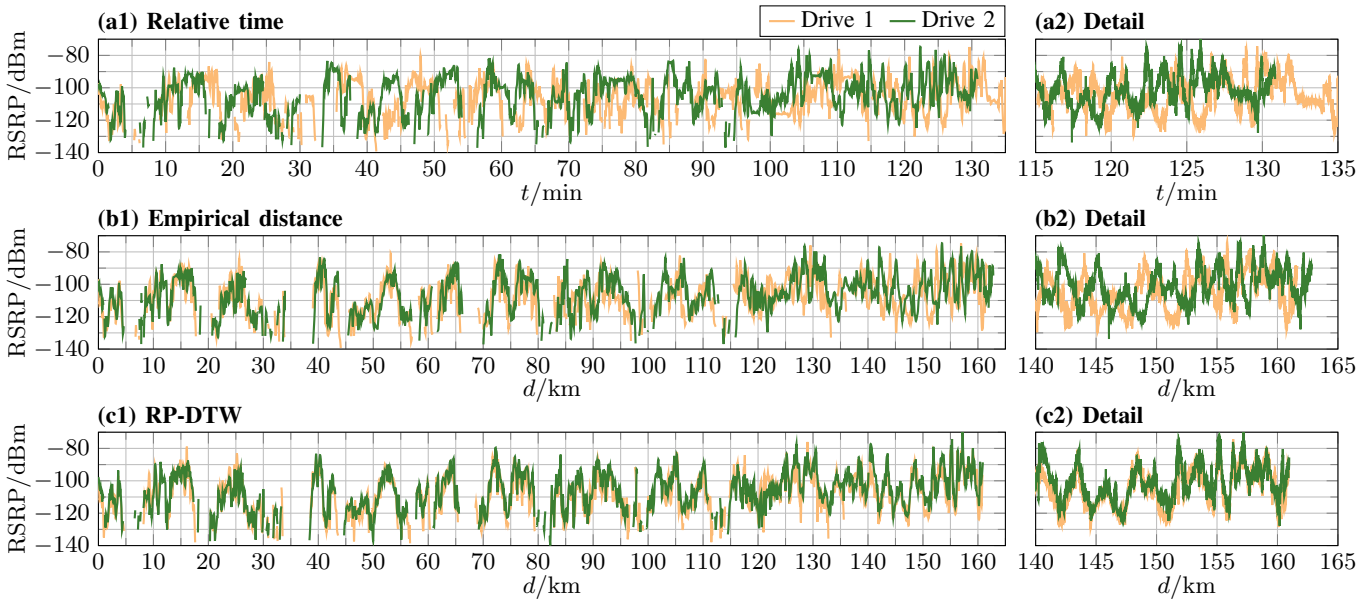

Fig. 2. Three different alignment methods applied to RSRP measurements in the LTE network of mobile network operator (MNO) A. (a) The same relative time stamps correspond to distinct locations in each drive due to different speed profiles (Fig. 1). (b) Calculating the traveled distance from GPS coordinates according to (1) causes small location error contributions to accumulate. The traces from different measurements thus drift apart slowly. (c) The modified dynamic time-warping algorithm with reference path (RP-DTW) successfully aligns the repeated measurements along the whole route.

Along path q, we measure a spatial function $\boldsymbol{f}\colon q \to \mathbb{R}^C$. Keeping in mind that the value of d identifies a specific point in $\mathbb{R}^D$, we can characterize $\boldsymbol{f}$ as a function of the distance d:

$$\boldsymbol{f}(d)\colon [0, d_{\max}] \to \mathbb{R}^C. \tag{3}$$

Any physical measuring device that travels along path q can collect only discrete samples that consist of the measured coordinates $\boldsymbol{x}_n \in \mathbb{R}^D$, relative time stamps $t_n \in \mathbb{R}^+$, and signal values $\boldsymbol{f}_n \in \mathbb{R}^C$. The measured locations may be biased and noisy; thus, it is possible that $\boldsymbol{x}_n \notin q$.

IV. Modified DTW with a Reference Path

Analogous to the classical DTW (Appendix A), we propose a modified dynamic time warping with a reference path (briefly, "reference path DTW," or RP-DTW) to align repeated spatial measurements.

We introduce a reference path p, which is a discretization of the continuous path (2). This reference path consists of $K+1$ locations $\boldsymbol{x}_{\mathrm{ref},k}$ and corresponding distances d_k:

$$p = ((\boldsymbol{x}_{\mathrm{ref},k},\, d_k))_{k=0}^{K}, \quad \boldsymbol{x}_{\mathrm{ref},k} = q(d_k). \tag{4}$$

We warp (align) the measured locations $\boldsymbol{x}_n$ with the reference locations $\boldsymbol{x}_{\mathrm{ref},k}$, thus assigning distances d_k to our measurement samples $(t_n, \boldsymbol{x}_n, \boldsymbol{f}_n)$.

In traditional DTW, the length of the output can differ in each pair of input sequences, which is undesirable when aligning multiple repetitions. Hence, we modify the DTW constraints to guarantee that all output sequences would have the same length. Fig. 3 illustrates the RP-DTW concept.

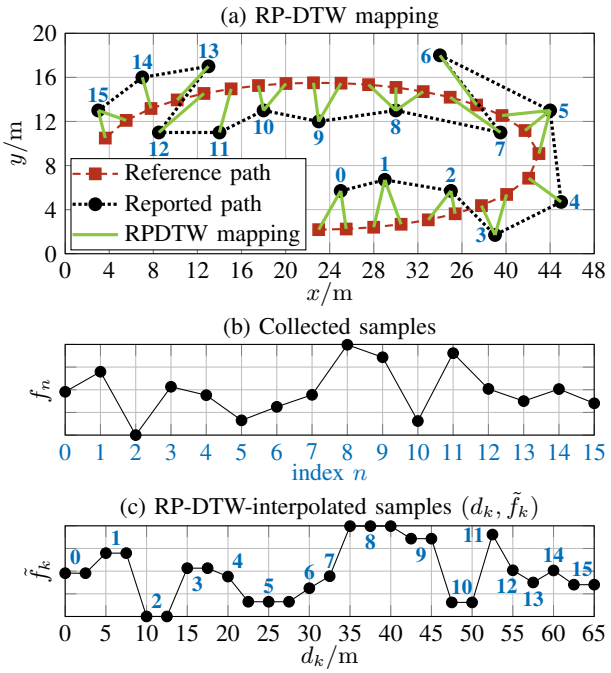

Fig. 3. RP-DTW algorithm. (a) A measurement took place along the reference path p. The reported path $(\boldsymbol{x}_n)_{n=0}^{N}$, e.g., recorded GPS coordinates, can significantly differ from p. The RP-DTW assigns exactly one location of the reported path to each location of the reference path. Each location of the reported path can be assigned to multiple locations of p. (b) Samples $\boldsymbol{f}_n$ are recorded at the same time as locations $\boldsymbol{x}_n$. (c) The RP-DTW mapping in (a) defines the interpolation of the samples $(\boldsymbol{f}_n)_{n=0}^{N} \to (\tilde{\boldsymbol{f}}_k)_{k=0}^{K}$. Each interpolated sample $\tilde{\boldsymbol{f}}_k$ corresponds to a different location on the reference path, and thus to a different distance d_k.

A. The RP-DTW Algorithm

RP-DTW is a mapping that transforms an input sequence of samples $(\boldsymbol{x}_n, \boldsymbol{f}_n)$ into an output sequence of samples $(\tilde{\boldsymbol{x}}_k, \tilde{\boldsymbol{f}}_k)$,

$$((\boldsymbol{x}_n, \boldsymbol{f}_n))_{n=0}^{N} \xrightarrow{\pi, p} ((\tilde{\boldsymbol{x}}_k, \tilde{\boldsymbol{f}}_k))_{k=0}^{K}, \tag{5}$$

according to the reference path p (4) and index path π.

The index path π consists of indexes $n_k \in \{0, \dots, N\}$ and defines the output samples as

$$\pi = (n_k)_{k=0}^{K} \quad \Rightarrow \quad \tilde{\boldsymbol{x}}_k = \boldsymbol{x}_{n_k}, \quad \tilde{\boldsymbol{f}}_k = \boldsymbol{f}_{n_k}. \tag{6}$$

The index path π fulfills the following constraints:

$$\text{start / end:} \quad n_0 = 0, \; n_K = N, \tag{7}$$

$$\text{allowed moves:} \quad \forall k \geq 1 \colon n_k \in \begin{cases} \{n_{k-1}, n_{k-1} + 1)\}, & n_k > 0, \\ \{n_{k-1}\}, & n_k = 0, \end{cases} \tag{8}$$

$$\text{optimality:} \quad \pi = \arg\min_{\pi' \in \mathcal{P}} \sum_{k=0}^{K} \delta(\tilde{\boldsymbol{x}}_k, \boldsymbol{x}_{\mathrm{ref},k}), \tag{9}$$

with an arbitrary distance function (or cost function) δ and a set $\mathcal{P}$ of all index paths π' that satisfy (6)–(8). Index path constraints (7) and (8) imply that the reference path p cannot have less elements than the measurement sequence: $K \geq N$.

B. Optimum Index Path and Complexity

The RP-DTW is, by definition (9), optimum in the sense that it minimizes the difference between the reference path $(\boldsymbol{x}_{\mathrm{ref},k})_{k=0}^{K}$ and the warped measured path $(\tilde{\boldsymbol{x}}_k)_{k=0}^{K}$ under the constraints (7), (8). Section IV-A lists all the properties that the resulting warped path has to fulfill but provides no specific recipe on how to find it.

Same as in Section A-A, we find the optimum index-path π by applying Bellman's principle of optimality [16] (in the context of finding the most likely sequence of hidden states known as the Viterbi algorithm [17]): The optimum (lowest cost) path among all possible paths from point A through B to C necessarily contains a subpath from A to B, which is the optimum path among all paths that lead from A to B.

We define the shorthand $\delta_{k,n} \coloneqq \delta(\tilde{\boldsymbol{x}}_{\mathrm{ref},k}, \boldsymbol{x}_n)$ and by applying Bellman's principle we recursively construct a path-cost-matrix $\boldsymbol{\Gamma}$ analogous to (18). Each element $\gamma_{k,n}$ is equal to the total cost of the cheapest partial path from $(0, 0)$ to (k, n) with respect to the allowed moves:

$$\gamma_{k,n} = \begin{cases} \delta_{k,n} + \min\{\gamma_{k-1,n}, \gamma_{k-1,n-1}\}, & k \geq n > 0, \\ \delta_{k,n} + \gamma_{k-1,n}, & n = 0, \\ \text{not defined}, & n > k. \end{cases} \tag{10}$$

The elements $\gamma_{k,n}$ with $n > k$ cannot be reached by the allowed moves (8) and are therefore undefined. The first element is initialized as $\gamma_{0,0} = \delta_{0,0}$. The total minimum distance in (9) thus equals $\gamma_{K,N}$.

We recursively find the optimum index path π by starting at the last index (K, N) and then repeatedly choosing the smaller of the two neighbors $\gamma_{k-1,l-1}$, $\gamma_{k-1,l}$ in each step until we reach the first index $(0, 0)$. The above-described construction of the cost-matrix $\boldsymbol{\Gamma}$ implies that the RP-DTW complexity is quadratic with respect to the number of path-samples.

C. Remarks

Index path π interpolates the input samples $\boldsymbol{f}_n$ into output samples $\tilde{\boldsymbol{f}}_k$, which correspond to locations $\boldsymbol{x}_{\mathrm{ref},k}$ and distances d_k of the reference path p [Fig. 3 (c)]. RP-DTW preserves the order, in which the locations of p are visited. For example, selecting the nearest $\{\boldsymbol{x}_{\mathrm{ref},k}\}_{k=0}^{K}$ for each $\boldsymbol{x}_n$ would not guarantee the order preservation [$n = 6$, $n = 7$ in Fig. 3 (a)].

Apart from the condition $K \geq N$, we did not specify the discretization $q \to p$. If we know the minimum speed[3] and maximum sampling frequency, we can calculate the shortest traveled distance between two samples; this distance we can apply to discretize q. Using a coarser discretization (small K), we lose the distance-resolution as the true location of $\boldsymbol{f}_n$ may be far from any reference location $\boldsymbol{x}_{\mathrm{ref},k}$. By using a finer discretization (large K), the interpolation [Fig. 3 (c)] repeats samples $\boldsymbol{f}_n$ multiple times.

V. Measurements

As mentioned in Section I-A, researchers often analyze overall performance through empirical distributions. By applying RP-DTW, we can examine the performance of each waypoint (as in [8], however, without the tedious requirement of maintaining a constant speed).

A. Setup

We conducted two repeated measurements between Vienna (railway station Franz-Josefs-Bahnhof) and Gmünd while onboard a Regional-Express train (ÖBB Cityjet). Both measurements took place on 16 February 2020: the first one between 16:28 and 18:45, the second one between 19:09 and 21:27.

We collected the LTE KPIs using Keysight's NEMO smartphones [19], which were placed on a train seat (Fig. 5) to capture the experience of real train passengers. In total, we had three active phones. Each phone was equiped with a SIM card of a different Austrian MNO. From the various KPIs collected, we focus on RSRP (as it remains most stable over time).

B. Results

The lowest LTE frequency we encountered was $800\,\mathrm{MHz}$. To avoid small-scale fading, we excluded all measurement samples with velocities lower than $10\,\mathrm{km/h}$ (channel coherence time $\approx 57\,\mathrm{ms}$). Since the sampling period of our measurement device is $500\,\mathrm{ms}$, the small-scale local minima and maxima thus effectively average out, and the measuring device captures only the large-scale trends (shadowing + path loss). For more details, see [18]. We obtained the coordinates of the reference path from OpenStreetMap [20], which we resampled to one-meter resolution.

We applied RP-DTW to align six traces in total—two repeated drives for each of the three MNOs (anonymized as A, B, C). The full RSRP traces of MNO A are depicted in Fig. 2. Full traces of MNOs B and C are not plotted in this paper as they are very similar to MNO A (Fig. 2). Instead, we offer all results as an online data set [1].

[3]Note that the measurement intervals with $v = 0$ should be excluded [18].

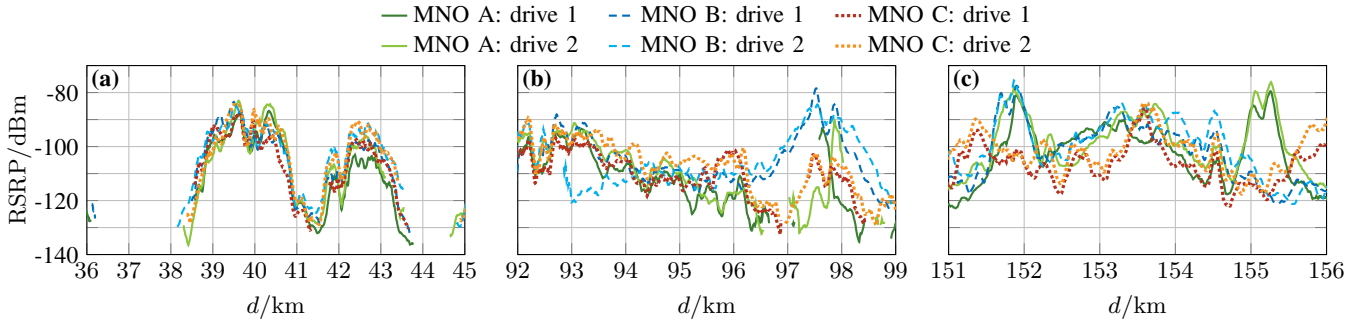

Fig. 4. RSRP traces aligned with RP-DTW: Zoomed-in details of interesting railway segments. Segments with missing traces have no LTE coverage.

Fig. 5. Our measurement setup: NEMO phones by Keysight placed on a train seat. During the campaign, three phones were active. Each phone was equipped with a SIM card of a different Austrian mobile network operator. The phones were locked to LTE.

To present a part of the data set, we show zoomed-in details of three railway segments in Fig. 4. Drive 1 and drive 2 of a single operator usually yield similar RSRP traces. In such a case, we can consider the measured values as reliable. (With tens of repeated drives, we could even estimate an RSRP distribution for each waypoint.)

We find an exception in plot (b) at 93–94 km, which contains an inconsistency between drive 1 and 2 of MNO B (e.g., due to different handovers). In such cases, we need to conduct more repetitions in order to asses the performance better.

In most of the areas, all three MNOs show the same performance [e.g., Fig. 4 (a)], which indicates that they share the same base station towers. Segments in plots (b) and (c) were chosen to present railway sections, where MNOs provide different coverage. In plot (b), at 96–99 km, MNO B offers better coverage than A and C. In plot (c), at 155–155.5 km, MNO A performs the best. Such analysis is useful for MNOs to identify the segments that need a coverage boost.

VI. Conclusion

In this paper, we have proposed a novel RP-DTW algorithm that warps the measured coordinates with a reference path and then applies the resulting warping indexes to the measured function values. By forbidding one of the three allowed moves in the index path of the classical DTW, we assure that every output-sequence has the same length as that of the reference path. This allows us to align multiple sequences successively—all of them end up on the same distance grid.

RP-DTW is optimal in the sense that it minimizes the total difference between the measured locations and the reference locations under a set of constraints. Compared to more straightforward distance estimations, RP-DTW processes all measured locations jointly, thus preventing distance errors from accumulating as the number of samples increases.

We have seen that RP-DTW can correct noisy location estimates. However, it cannot deal with an absence of location samples (e.g., loss of GPS signal in tunnels). In such cases, we would have to make assumptions about the vehicle's speed in the non-covered segments and, for example, interpolate the missing coordinates.

In the presented measurements, the GPS errors were rather small. In future work, we will evaluate the performance of RP-DTW in simulations to examine the impact of location error magnitude in more detail. We also plan to offer a more detailed comparison with other alignment methods.

Acknowledgment

This work has been funded by the ITC, TU Wien. The research has been cofinanced by the Austrian FFG, Bridge Project No. 871261. We thank A1 Telekom Austria AG for their support and Kei Cuevas for the proofreading.

References

[1] V. Raida *et al.* (2020) RP-DTW data set. [Online]. Available: http://doi.org/10.23728/b2share.b7f93ada6c6f46b296cd3c39665982c4

[2] P. Senin, "Dynamic time warping algorithm review," University of Hawaii at Manoa, Tech. Rep., 2008.

[3] C. A. Ratanamahatana and E. Keogh, "Everything you know about dynamic time warping is wrong," in *Proc. 3rd Workshop on Mining Temporal and Sequential Data*, Jan. 2004.

[4] X. Xi, E. Keogh, C. Shelton, L. Wei, and C. A. Ratanamahatana, "Fast time series classification using numerosity reduction," in *Proc. 23rd Int. Conf. Mach. Learn.*, ser. ICML '06. New York, NY, USA: ACM, 2006, pp. 1033–1040.

[5] A. Bagnall, A. Bostrom, J. Large, and J. Lines, "The great time series classification bake off: An experimental evaluation of recently proposed algorithms. extended version," 2016.

[6] F. Petitjean, G. Forestier, G. I. Webb, A. E. Nicholson, Y. Chen, and E. Keogh, "Dynamic time warping averaging of time series allows faster and more accurate classification," in *2014 IEEE Int. Conf. Data Mining*, Dec. 2014, pp. 470–479.

[7] F. Petitjean, A. Ketterlin, and P. Gançarski, "A global averaging method for dynamic time warping, with applications to clustering," *Pattern Recogn.*, vol. 44, no. 3, pp. 678–693, Mar. 2011.

[8] V. Raida, P. Svoboda, M. Lerch, and M. Rupp, "Repeatability for spatiotemporal throughput measurements in LTE," in *2019 IEEE 89th Vehicular Technology Conference (VTC2019-Spring)*, 2019.

[9] G. Sezgin, Y. Coskun, E. Basar, and G. K. Kurt, "Performance evaluation of a live multi-site LTE network," *IEEE Access*, vol. 6, 2018.

[10] R. Irmer, H. Mayer, A. Weber, V. Braun, M. Schmidt, M. Ohm, N. Ahr, A. Zoch, C. Jandura, P. Marsch, and G. Fettweis, "Multisite field trial for LTE and advanced concepts," *IEEE Commun. Mag.*, vol. 47, no. 2, 2009.
[11] V. Sevindik, J. Wang, O. Bayat, and J. Weitzen, "Performance evaluation of a real long term evolution (LTE) network," in *37th IEEE LCN Conf.*, 2012.
[12] J. Beyer, J. Belschner, J. Chen, O. Klein, R. Linz, J. Muller, Y. Xiang, and X. Zhao, "Performance measurement results obtained in a heterogeneous LTE field trial network," in *77th VTC Spring*, 2013.
[13] M. P. Wylie-Green and T. Svensson, "Throughput, capacity, handover and latency performance in a 3GPP LTE FDD field trial," in *GLOBECOM 2010*, 2010.
[14] J. Landre, Z. E. Rawas, and R. Visoz, "LTE performance assessment prediction versus field measurements," in *IEEE 24th PIMRC*, 2013.
[15] 3GPP, "Physical layer; measurements," TS 36.214, 2018, version 15.2.0.
[16] R. Bellman, *Dynamic Programming*, 1st ed. Princeton, NJ, USA: Princeton University Press, 1957.
[17] A. Viterbi, "Error bounds for convolutional codes and an asymptotically optimum decoding algorithm," *IEEE Transactions on Information Theory*, vol. 13, no. 2, 1967.
[18] V. Raida, P. Svoboda, and M. Rupp, "On inappropriateness of static measurements for benchmarking in wireless networks," in *2020 IEEE 91th Veh. Technol. Conf.*, Jun. 2020, accepted for publication. [Online]. Available: https://owncloud.nt.tuwien.ac.at/index.php/s/46q7xq734RTd5Zq
[19] Keysight Technologies. (2020) Nemo Handy handheld measurement solution. [Online]. Available: https://www.keysight.com/en/pd-2767485-pn-NTH00000A/nemo-handy
[20] V. Raida. Export waypoints from OSM. [Online]. Available: https://github.com/vraida/Export-waypoints-from-OpenStreetMap

APPENDIX A
THE CLASSICAL DYNAMIC TIME WARPING

The DTW is a mapping that transforms a pair of sequences of (possibly) different lengths into a new pair of sequences that both have the same length:

$$\big((\boldsymbol{a}_l)_{l=0}^{L}, (\boldsymbol{b}_n)_{n=0}^{N}\big) \xrightarrow{\pi} \Big((\tilde{\boldsymbol{a}}_k)_{k=0}^{K}, (\tilde{\boldsymbol{b}}_k)_{k=0}^{K}\Big), \quad \boldsymbol{a}_l, \boldsymbol{b}_n, \tilde{\boldsymbol{a}}_k, \tilde{\boldsymbol{b}}_k \in \mathbb{R}^D,\ D \in \mathbb{Z}^+. \tag{11}$$

The mapping is defined by the sequence π ("index path"),

$$\pi = ((l_k, n_k))_{k=0}^{K}, \quad l_k \in \{0, \dots, L\},\ n_k \in \{0, \dots, N\}, \tag{12}$$

as follows:

$$\tilde{\boldsymbol{a}}_k = \boldsymbol{a}_{l_k}, \quad \tilde{\boldsymbol{b}}_k = \boldsymbol{b}_{n_k}. \tag{13}$$

The index path fulfills the following constraints:

$$\text{first element:} \quad (l_0, n_0) = (0, 0), \tag{14}$$

$$\text{last element:} \quad (l_K, n_K) = (L, N), \tag{15}$$

$$\text{allowed moves:} \quad \text{[Equation in the footnote]}, \tag{16}$$

$$\text{optimality:} \quad \pi = \arg\min_{\pi' \in \mathcal{P}} \sum_{k=0}^{K} \delta(\tilde{\boldsymbol{a}}_k, \tilde{\boldsymbol{b}}_k), \tag{17}$$

with a distance function[4] δ and set $\mathcal{P}$ that contains all paths π' (of various lengths), which are consistent with (11)–(16). Due to constraints (14)–(16), the output sequences cannot be shorter than the input sequences: $K \geq \max\{L, N\}$. Fig. 6 shows the warping of two scalar sequences ($D = 1$) according to an index path π visualized in an index matrix.

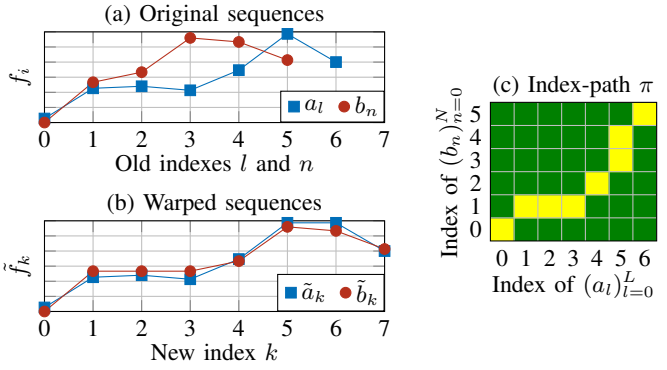

Fig. 6. The sequences $(a_l)_{l=0}^{L}$, $(b_n)_{n=0}^{N}$ of lengths $L+1=7$, $N+1=6$ [plot (a)] are warped to the new sequences $(\tilde{a}_k)_{k=0}^{K}$, $(\tilde{b}_k)_{k=0}^{K}$ of the same length $K+1=8$ [plot (b)] according to the index path π [plot (c)].

The index path always begins in the lower left corner (14) and ends in the upper right corner (15). From the start point, we can get to the end point by successively applying one of the three[5] allowed moves (16): one step to the right, one step up, or one step diagonally (northeast). From all paths $\pi' \in \mathcal{P}$ that fulfill (14)–(16), the selected path π is the one that minimizes the total distance of the warped output sequences (17).

A. Finding the Optimum Index Path

We can express the total distance of the warped sequences in terms of the original sequences: $\sum_{k=0}^{K} \delta(\boldsymbol{a}_{l_k}, \boldsymbol{b}_{n_k})$. We use the shorthand $\delta_{l,n} = \delta(\boldsymbol{a}_l, \boldsymbol{b}_n)$, and we define the path-cost-matrix $\boldsymbol{\Gamma}$ with elements $\gamma_{0,0} = \delta_{0,0}$ and $\gamma_{l,n\neq(0,0)}$:

$$\gamma_{l,n} = \begin{cases} \delta_{l,n} + \min\{\gamma_{l-1,n}, \gamma_{l,n-1}, \gamma_{n-1,n-1}\}, & l, n > 0, \\ \delta_{l,n} + \gamma_{l-1,n}, & n = 0, \\ \delta_{l,n} + \gamma_{l,n-1}, & l = 0. \end{cases} \tag{18}$$

By the definition (18), each element $\gamma_{l,n}$ is equal to the total cost of the cheapest partial path from $(0,0)$ to (l,n) with respect to the allowed moves in (16). Depending on which of the three neighbors of $\gamma_{l,n}$ is smallest, we know that the cheapest path comes to $\gamma_{l,n}$ either from left, from below, or from southwest.

After calculating all elements of $\boldsymbol{\Gamma}$ (quadratic complexity), we start in the upper right corner (L, N) and then reconstruct the optimum path by following the cheapest of the three allowed neighbors $\{\gamma_{l-1,n}, \gamma_{l,n-1}, \gamma_{n-1,n-1}\}$ at every step, until we reach the lower left corner $(0,0)$. Note that $\gamma_{L,N}$ is equal to the total distance of the optimum path.

$$\forall k \in \{1, \dots, K\}\colon\ (l_k, n_k) \in \begin{cases} \{(l_{k-1}+1, n_{k-1}), (l_{k-1}, n_{k-1}+1), (l_{k-1}+1, n_{k-1}+1)\}, & l_k > 0 \wedge n_k > 0, \\ \{(l_{k-1}+1, n_{k-1})\}, & l_k > 0 \wedge n_k = 0, \\ \{(l_{k-1}, n_{k-1}+1)\}, & l_k = 0 \wedge n_k > 0. \end{cases} \tag{16}$$

[4]For example, Euclidian distance $\delta(\tilde{\boldsymbol{a}}_k, \tilde{\boldsymbol{b}}_k) = \|\tilde{\boldsymbol{a}}_k - \tilde{\boldsymbol{b}}_k\|_2$.
[5]With the exception of the first row $l_k = 0$ and first column $n_k = 0$.